Molecular Cell
Article

Genome-wide Functional Annotation of Dual-Specificity Protein- and Lipid-Binding Modules that Regulate Protein Interactions

Yong Chen,[1,8] Ren Sheng,[1,8] Morten Källberg,[2,8] Antonina Silkov,[4,8] Moe P. Tun,[1] Nitin Bhardwaj,[2] Svetlana Kurilova,[1] Randy A. Hall,[5] Barry Honig,[3,4] Hui Lu,[2,6,*] and Wonhwa Cho[1,7,*]
[1]Department of Chemistry
[2]Department of Bioengineering
University of Illinois at Chicago, Chicago, IL 60607, USA
[3]Howard Hughes Medical Institute
[4]Department of Biochemistry and Molecular Biophysics and Center for Computational Biology and Bioinformatics
Columbia University, New York, NY 11032, USA
[5]Department of Pharmacology, Emory University School of Medicine, Atlanta, GA 30322, USA
[6]Shanghai Institute of Medical Genetics, Children Hospital of Shanghai, Shanghai Jiaotong University, Shanghai 200240, China
[7]Division of Integrative Biosciences and Biotechnology, Pohang University of Science and Technology, Pohang 790-784, Korea
[8]These authors contributed equally to this work
*Correspondence: wcho@uic.edu (W.C.), huilu@uic.edu (H.L.)
DOI 10.1016/j.molcel.2012.02.012

SUMMARY

Emerging evidence indicates that membrane lipids regulate protein networking by directly interacting with protein-interaction domains (PIDs). As a pilot study to identify and functionally annodate lipid-binding PIDs on a genomic scale, we performed experimental and computational studies of PDZ domains. Characterization of 70 PDZ domains showed that ~40% had submicromolar membrane affinity. Using a computational model built from these data, we predicted the membrane-binding properties of 2,000 PDZ domains from 20 species. The accuracy of the prediction was experimentally validated for 26 PDZ domains. We also subdivided lipid-binding PDZ domains into three classes based on the interplay between membrane- and protein-binding sites. For different classes of PDZ domains, lipid binding regulates their protein interactions by different mechanisms. Functional studies of a PDZ domain protein, rhophilin 2, suggest that all classes of lipid-binding PDZ domains serve as genuine dual-specificity modules regulating protein interactions at the membrane under physiological conditions.

INTRODUCTION

Regulation of cellular processes, such as cell signaling, involves myriad protein-protein interactions that are typically mediated by modular protein-interaction domains (PIDs), such as SH2, SH3, PDZ, and WW domains (Bhattacharyya et al., 2006; Pawson, 2004; Pawson and Nash, 2003). Cellular membranes, including the plasma membrane (PM), offer unique local environments that facilitate protein-protein interactions and therefore serve as the main sites for protein complexes and networks (Bray, 1998; Cho, 2006). Accumulating evidence suggests that membrane lipids play a key role in protein complex formation or networking through direct interactions with signaling proteins, scaffold proteins in particular (Cho, 2006; Winters et al., 2005). Membrane recruitment of cellular proteins is mediated by lipid-binding domains or motifs that either recognize specific lipids or nonspecifically interact with the anionic membrane surface (Cho and Stahelin, 2005; DiNitto et al., 2003; Lemmon, 2008). Thus, it has been generally thought that the protein networking and interactions at the membrane involve the coordinated action of separate lipid-binding domains (or motifs) and PIDs in the same molecules (Di Paolo and De Camilli, 2006; Lemmon, 2008). Recent studies have shown, however, that PIDs, such as PDZ domain (Feng and Zhang, 2009; Zimmermann, 2006) and PTB domain (Ravichandran et al., 1997; Zhou et al., 1995), can directly interact with membrane lipid(s) and thus mediate both protein-protein and protein-lipid interactions. It has also been reported that some lipid-binding domains, such as the PH domain (Yao et al., 1994) and the PX domain (Lee et al., 2006), can interact with proteins as well as lipids. These findings suggest that PIDs and lipid-binding domains may serve as dual-specificity lipid- and protein-binding modules that play a crucial role in protein interactions and networking. To test this hypothesis, we have developed new experimental and bioinformatics tools for the identification and characterization of dual-specificity PIDs on a genomic scale and applied these tools to the study of PDZ domains.

The PDZ domain is a small (~90 amino acid) modular PID that interacts with a short C-terminal sequence of its target protein(s) (Feng and Zhang, 2009; Sheng and Sala, 2001). The domain was originally identified in three unrelated proteins, postsynaptic density 95 (PSD95), disc large 1 (DLG1), and zonular occludens 1 (ZO1), but has since been found in a large number of proteins,

including postsynaptic proteins and cell junction proteins. A SMART search (Schultz et al., 1998) in genomic mode identifies 148 human proteins containing >500 different PDZ domains, making them one of the most ubiquitous PIDs in vertebrates. Most PDZ domain-containing proteins contain multiple copies of PDZ domains, serving as prototype scaffold proteins that reversibly interact with multiple binding partners, thereby dynamically coordinating signaling complex formation and protein networking (Feng and Zhang, 2009; Sheng and Sala, 2001). Recent studies have shown that PDZ domains can directly interact with anionic model membranes and that in some cases this PDZ-membrane interaction is important for the cellular function of their host proteins (Meerschaert et al., 2009; Pan et al., 2007; Wu et al., 2007; Zimmermann et al., 2002). However, it is still not known if lipid binding is a general property of PDZ domains, if they can serve as authentic dual-specificity modules under physiological conditions, and how their protein and lipid binding are interrelated. Thus, the PDZ domain is an excellent candidate for the pilot study for the genome-wide identification and characterization of dual-specificity PIDs.

RESULTS

SPR Analysis of 70 Mammalian PDZ Domains

A recent study measured the binding of 74 PDZ domains to anionic vesicles by vesicle pelleting assay (Wu et al., 2007). Although the study revealed a high tendency of PDZ domains to bind lipids, the qualitative nature of the data limits their application to systematic analysis (or prediction) of membrane-binding properties of PDZ domains and of the interplay between their membrane and protein interactions. It was therefore necessary to collect a robust quantitative database large enough for statistical and systematic analysis. All reported membrane-binding PDZ domains bind anionic membranes with low to no lipid head group specificity (Meerschaert et al., 2009; Pan et al., 2007; Wu et al., 2007; Zimmermann et al., 2002). Also, a majority of PDZ domain proteins interact with protein partners that are associated with the PM (Feng and Zhang, 2009; Sheng and Sala, 2001) whose inner (i.e., cytoplasmic) layer is highly anionic due to the presence of phosphatidylserine (PS) and phosphatidylinositiol-4,5-bisphosphate (PtdIns[4,5]P_2) (Cho and Stahelin, 2005; McLaughlin and Murray, 2005). Thus, PDZ domains are most likely to interact with the inner layer of PM. For this reason we used the vesicles whose lipid composition recapitulates that of inner PM (i.e., PM-mimetic vesicles) (Cho and Stahelin, 2005) as a model membrane and rigorously determined the K_d values for 70 monomeric PDZ domains from 35 different mammalian proteins by surface plasmon resonance (SPR) analysis (Cho et al., 2001). We mainly selected uncharacterized PDZ domains (i.e., 51) for this study but also reevaluated some previously characterized PDZ domains (i.e., 19) (Wu et al., 2007) to directly compare the results from the two different analyses.

As shown in Table 1, 27 out of 70 tested PDZ domains (~40%) have submicromolar K_ds for the PM vesicles with the highest affinity in the range of 10^{-8} M, which is comparable to that of canonical lipid-binding domains (Cho and Stahelin, 2005). Syntenin1 PDZ domains (Zimmermann et al., 2002) and the second PDZ domain of ZO1 (Meerschaert et al., 2009), which were reported to have physiologically significant membrane affinity, have 1–3 μM K_ds under our experimental conditions (see Table 1). Our results thus indicate that membrane binding is a more general property of PDZ domains than previously thought and might play a role in their cellular localization (see Figure S1 online) and/or function. Table 1 also shows a significant discrepancy between our data and the previous results (Wu et al., 2007). In particular, 5 (out of 17) PDZ domains that were previously classified as nonmembrane binder turned out to bind PM-mimetic vesicles with K_d = 140–930 nM. For those PDZ domains with submicromolar affinity for the PM vesicles, we also measured the selectivity for phosphoinositides (PtdIns*P*), and most PDZ domains did not show appreciable PtdIns*P* selectivity. To validate our SPR data, we also determined K_d values for selected PDZ domains by a fluorescence resonance energy transfer (FRET) assay (see Table S1 and Figure S2). Results show that K_d values determined by the two different methods are comparable.

Classification Model for Predicting Membrane-Binding Affinity of PDZ Domains

A significant percentage of membrane-binding PDZ domains in our data set allowed us to build a high-accuracy prediction model for other PDZ domains. The PDZ domains in general have a high degree of sequence similarity (Feng and Zhang, 2009; Sheng and Sala, 2001). However, our data show that sequence similarity between any two PDZ domains does not translate into similar membrane-binding properties, making it a poor indicator for classification and prediction purposes. This is in contrast to other lipid-binding domains, such as the FYVE domain, for which a good correlation between sequence similarity and relative membrane affinity was observed (Blatner et al., 2004). Therefore, it was necessary to build a more sophisticated model based on quantification of physical and chemical characteristics of the domains.

We recently developed a machine learning-based prediction method for membrane-binding domains that uses a numerical vector representation obtained from primary and tertiary structures of proteins as input features and various machine learning algorithms as classifiers (Bhardwaj et al., 2006). To apply this method to our current task of discriminating membrane-binding properties among highly homologous PDZ domains, we incorporated residue-specific features derived from the domain sequence data in addition to the previously used protein-level features from structural data. Protein-level features enabling a domain to interact with membranes include nonspecific electrostatic attraction between anionic membranes and basic protein residues (Mulgrew-Nesbitt et al., 2006), association of hydrophobic protein residues with the membrane hydrocarbon core (Stahelin et al., 2003), and hydrogen bonds between key protein residues and lipid head groups (Cho and Stahelin, 2005). To incorporate residue-specific features, we determined the score of each residue and the cumulative score for a segment around it (Park et al., 2008) by calculating the recursive functional classification (RFC) matrix. This statistical scoring approach helps identify residues that are more likely to be observed at

Table 1. The Membrane Binding Affinity of the 70 Experimentally Tested PDZ Domains Used for Training the Classification Model

Gene	Species	Residue Number	K_d (nM) for PM	PtdIns*P* Selectivity	Results from Wu et al. (2007)
NHERF1/EBP50-PDZ1	human	10–98	24 ± 1[a]	low[c]	
Dvl2-PDZ	human	261–353	33 ± 3	PtdIns(4,5)P_2	
Dvl1-PDZ	human	245–337	45 ± 6		
Dvl3-PDZ	human	243–335	50 ± 5	PtdIns(4,5)P_2	
Tamalin-PDZ	mouse	100–186	90 ± 8	low	
SAP102-PDZ3	rat	404–482	140 ± 5	PtdIns(4,5)P_2	no binding
				PtdIns(3,4,5)P_3	
LNX1-PDZ4	mouse	638–721	180 ± 40	low	
PDZK2-PDZ3	mouse	263–343	280 ± 50	low	
MAGI1-PDZ5	human	998–1,091	290 ± 10	low	
PDZ-GEF-PDZ	human	385–470	290 ± 32	low	
β2-syntrophin-PDZ1	human	115–195	320 ± 80	low	
PDZK2-PDZ2	mouse	151–255	320 ± 32	low	
nNOS-PDZ	human	17–96	340 ± 10	low	
PSD95-PDZ3	rat	313–391	390 ± 30	low	no binding
INADL-PDZ6	human	1,068–1,160	480 ± 190	low	
Chapsyn110-PDZ3	rat	421–499	510 ± 50	low	
γ2-syntrophin-PDZ	mouse	73–153	530 ± 140	low	
Harmonin-PDZ1	mouse	87–165	600 ± 70	low	
MAGI3-PDZ5	human	1,021–1,100	610 ± 190	low	no binding
SAP97-PDZ3	rat	465–543	620 ± 70	PtdIns(3,4)P_2	no binding
LNX2-PDZ1	mouse	232–314	670 ± 100	low	
MAGI-2-PDZ3	human	605–683	750 ± 170	low	
α-syntrophin-PDZ1	mouse	81–161	860 ± 70	low	binding
MAGI-2 –PDZ5	human	920–1,007	900 ± 170	low	
PSD95-PDZ2	rat	160–244	930 ± 120	low	no binding
PDZ-PhoGEF-PDZ1	human	47–120	950 ± 110	low	
LNX1-PDZ1	mouse	278–360	960 ± 120	low	
ZO-1 PDZ-2	mouse	186–261	980 ± 200	PtdIns(3,4)P_2	binding
				PtdIns(3,4,5)P_3	
				PtdIns(4,5)P_2	
INADL-PDZ5	human	686–772	1070 ± 110		
β1-syntrophin-PDZ1	human	538–613	1440 ± 180		
Rhophilin-1-PDZ1	mouse	111–191	1440 ± 160		
Syntenin1-PDZ1	human	100–195	2200 ± 250		binding
SAP102-PDZ1	rat	149–233	4980 ± 870		
PSD95-PDZ1	rat	65–149	NM[b]		no binding
MAGI-2-PDZ2	human	426–492	NM		
MAGI-2-PDZ4	human	778–859	NM		
SAP97-PDZ1	rat	224–308	NM		no binding
Spinophilin-PDZ1	rat	496–581	NM		
Neurabin-PDZ1	rat	505–590	NM		no binding
NHERF-1-PDZ2	human	150–235	NM		
NHERF-2-PDZ2	human	150–230	NM		no binding
NHERF-2-PDZ1	human	11–88	NM		
SAP97-PDZ2	rat	318–402	NM		no binding
CAL-PDZ1	human	288–368	NM		
PDZK1-PDZ3	mouse	243–320	NM		

Table 1. *Continued*

Gene	Species	Residue Number	K_d (nM) for PM	PtdIns*P* Selectivity	Results from Wu et al. (2007)
PDZK1-PDZ1	mouse	9–87	NM		
MAGI-1-PDZ1	human	295–401	NM		
MAGI-1-PDZ3	human	643–720	NM		
MALS-1-PDZ1	human	108–187	NM		
E6TP1-PDZ1	human	953–1,025	NM		
LNX1-PDZ3	mouse	508–591	NM		
LNX1-PDZ2	mouse	385–465	NM		
Densin-180-PDZ1	rat	1,403–1,493	NM		
MAGI-2-PDZ1	human	17–98	NM		
MALS-3-PDZ1	mouse	93–172	NM		
LNX2-PDZ2	mouse	338–418	NM		
MAGI-1-PDZ2	human	472–554	NM		
PDZK2-PDZ4	mouse	394–472	NM		
Harmonin-PDZ2	mouse	211–289	NM		
MAGI-3-PDZ1	human	410–476	NM		
MAGI-3-PDZ3	human	726–807	NM		no binding
MAGI-3-PDZ4	human	851–935	NM		no binding
PDZK1-PDZ2	mouse	128–215	NM		
MUPP1-PDZ6	mouse	996–1,077	NM		
MUPP1-PDZ7	mouse	1,139–1,231	NM		no binding
MUPP1-PDZ8	mouse	1,338–1,421	NM		no binding
MUPP1-PDZ12	mouse	1,847–1,933	NM		no binding
MUPP1-PDZ13	mouse	1,972–2,055	NM		no binding
MAGI-3-PDZ2	human	578–641	NM		

[a]Mean ±SD values determined by SPR analysis using PM-mimetic vesicles.
[b]Not measurable by SPR analysis with up to 10 μM protein (i.e, K_d >10 μM).
[c]Determined by measuring the relative affinity for POPC/PtdInsP (97:3) by SPR analysis.

certain positions in membrane-binding PDZ domains than in nonbinding PDZ domains. Figure 1 depicts an example of this scoring procedure, displaying the score of each residue and the cumulative score for the neighboring segment of the rat PSD95-PDZ3 domain. It is evident that certain residues (i.e., R1, H5, T9, E19, D37, L38, S39, E40, and Q72) have strong influence on membrane binding of the domain. Interestingly, these residues are not exclusively located in the electrostatically positive region, which is generally involved in binding to anionic membranes, but in both electropositive and -negative regions. This pattern is also seen with several other membrane-binding PDZ domains. Among those residues found in the electronegative region, some residues (e.g., E and D) may form specific hydrogen bonds with lipids, as seen with PH domains (DiNitto and Lambright, 2006), while others may play indirect roles, such as guiding the membrane-binding orientation of the domain. It should be noted that the identity and the relative contribution of membrane-binding residues vary significantly among similar PDZ domains. This is demonstrated in residue and cumulative scoring plots for three different PDZ domains, SAP102-PDZ3, rhophilin 2-PDZ, and tamalin-PDZ (see Figure S3). A few high-scoring residues make a predominant contribution for SAP102-PDZ3, whereas many residues contribute relatively evenly to membrane binding for tamalin and rhophilin 2-PDZ domains.

We also optimized the classification method for the prediction of membrane-binding PDZ domains. To develop a binary classification method, one needs to define positive and negative cases. Since PDZ domains have a wide range of continuous K_d values, it was necessary to choose a specific K_d value as a threshold for physiologically significant membrane binding. In general, it is not straightforward to predict the cellular membrane binding of a particular protein from its K_d value for a model membrane. It is because membrane binding of a protein is different from chemical binding of two species with well-defined binding sites (White et al., 1998) and because it is technically challenging to accurately determine the cellular lipid concentrations (Yoon et al., 2011). We have thus taken a combinatorial approach of determining the relative membrane affinity (i.e., in terms of relative K_d) of a family of proteins by the SPR analysis and then measuring their cellular membrane-binding properties to estimate the threshold K_d value for their cellular membrane binding (Blatner et al., 2004; Cho and Stahelin, 2005). Since syntenin1-PDZ and ZO1-PDZ2, whose membrane affinity is physiologically significant (Meerschaert et al., 2009; Zimmermann et al., 2002), have 1–3 μM K_ds, we set the threshold K_d of PDZ domains

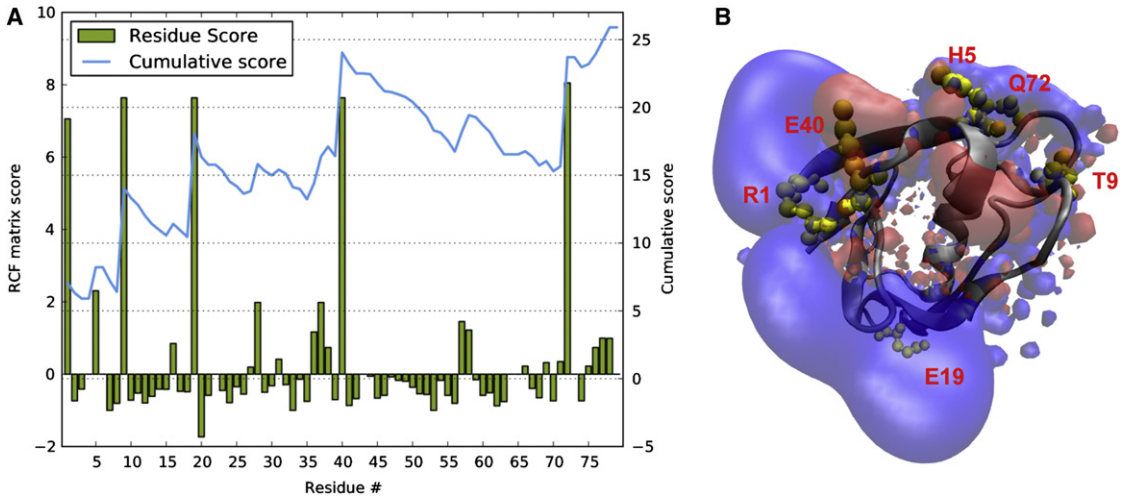

Figure 1. Quantification of Residue-Specific Features

(A) Residue and cumulative score obtained from the RFC matrix for the third PDZ domain of PSD95.

(B) The structure of the domain along with electrostatic isosurfaces. Key membrane-binding residues identified by the scoring system are highlighted and labeled.

to 1 μM. This threshold value divided our SPR-tested PDZ domains into 27 binding cases and 41 nonbinding cases. Lowering the cutoff K_d value to 0.5 μM would reduce the positive cases to 15. For evaluation of prediction, we tested two machine learning algorithms that have proven successful in diverse classification applications (Bhardwaj et al., 2005, 2006), i.e., the kernel-based support vector machine (SVM) methodology and the decision tree algorithm C4.5 combined with the boosting algorithm AdaBoost (referred to as ABC4.5). Table S2 summarizes the results from these algorithms with 10-fold crossvalidations and with different feature sets. The prediction was more accurate when structural and sequence features are used in combination than independently. Between the two algorithms, the SVM did well on both the 0.5 and 1 μM K_d cutoff data sets (see also Figure S4). Also, SVM algorithm achieved better accuracy (94%) with balanced sensitivity and selectivity with 1 μM K_d-cutoff. We thus decided to use SVM with all features and K_d = 1 μM as a threshold for the genome-wide prediction of membrane-binding activity of PDZ domains.

Predictions for 2,000 PDZ Domains from 20 Different Species

Using our optimized protocol, we predicted the membrane-binding properties of all 2,000 PDZ domains found in 20 different species. Since we used both structural and sequence features, domains included in our prediction are from all sequences for which reliable homology models could be generated (Supplemental Experimental Procedures). As seen in Figure 2, ~30% of PDZ domains are predicted to have submicromolar membrane-binding affinity, although some degree of variation is found among species. It thus seems evident again that membrane binding is a common property among PDZ domains. The complete collection of the PDZ domains annotated in this study can be found in our online resource MeTaDoR (Membrane Targeting Domains Resource) (http://metador.bioengr.uic.edu/) (Bhardwaj et al., 2007). Several options for searching the collection are given, among them host protein name, organism, and binding annotation. There is also an option to classify the domains with variable threshold K_d values. For each domain, the host protein and the domain location in the host protein are given, along with relevant links to public databases.

Experimental Validation of Prediction

To further validate our prediction model, we selected 25 PDZ domains from the list of 2,000 predictions and measured their membrane binding by SPR analysis. As with the initial screening of PDZ domains, we mainly selected uncharacterized PDZ domains for validation with the addition of a few PDZ domains previously characterized (Wu et al., 2007). Table 2 compares the experimental results, with our prediction values obtained using 1 μM K_d cutoff. All the binding cases were classified correctly, while three nonbinding cases were classified as binding ones. Thus the overall accuracy on the test set is ~90%, which is similar to the crossvalidation accuracy. Even the three misclassified cases for nonbinding PDZ domains (i.e., ZO-2-PDZ2, PAR3-PDZ1, and ZO-3-PDZ2) were borderline, low-confidence cases with prediction values $\leq$0.1, with 0 being the cut-off score separating binding and nonbinding domains. In particular, ZO-2-PDZ2 was predicted to be a membrane binder, while the experimental K_d value (i.e., 1.2 ± 0.4 μM) is only slightly above the 1 μM K_d threshold. Collectively, this evaluation demonstrates the accuracy and reliability of our prediction. The selection of 70 domains used for the initial database and 25 domains used for evaluation did not bias the outcome of our prediction: i.e., when PDZ domains in the two groups were interchanged, essentially the same results were obtained in terms of classification and prediction accuracy.

Functional Classification of Membrane-Binding PDZ Domains

To systematically analyze the location of membrane-binding sites and the interplay between membrane and protein-binding

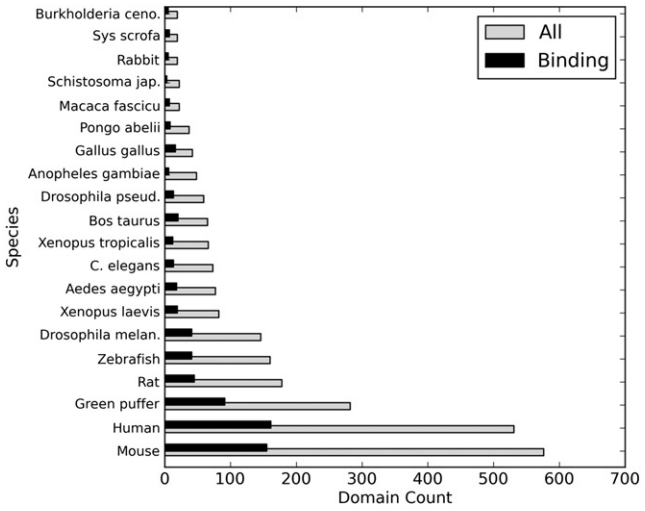

Figure 2. Membrane-Binding Statistics for 2,000 PDZ Domains Found in 20 Species

Predicted number of membrane-binding PDZ domains is shown for each species. SVM classifier was used for prediction with all features included and K_d = 1 μM as a threshold.

sites, we calculated the surface electrostatic potential for all mammalian PDZ domains using either known structures or best homology model structures (see the Supplemental Experimental Procedures). This analysis revealed that most of these PDZ domains have at least one prominent surface cationic patch that may serve as an anionic lipid-binding site. Depending on the location of the cationic patch in relation to the canonical peptide-binding site, they could be subdivided into two classes. Class A PDZ domains have a main cationic patch (or two largest patches, in the case that two or more patches are found), with no topological overlap with the peptide-binding site (see Figure S5), whereas class B PDZ domains contain the cationic patch proximal to the peptide pocket (Figure S6). We reasoned that this structural classification has functional implications because the prominent cationic patch in each PDZ domain is likely to represent its lipid-binding site. To test this hypothesis, we experimentally determined the location of lipid-binding sites and the interplay between their lipid and protein binding for selected members of each class.

Among class A PDZ domains, we selected the SAP102-PDZ3 that has a prominent cationic patch (R449, R459, and R484) in the opposite side of the peptide-binding pocket (Figure 3A). Interestingly, this cationic patch also forms a groove, suggesting that it may specifically bind a lipid head group. Our SPR analysis confirmed that this PDZ domain has definite selectivity for PtdIns(4,5)P_2 and PtdIns(3,4,5)P_3 over other PtdIns*P*s (Figure S7A), shows PtdIns(4,5)P_2 dependency in membrane binding (Figure S7B), and binds soluble inositol 1,4,5-trisphosphate (Ins[1,4,5]P_3) (Figure S8). Also, mutations of cationic residues in the groove (e.g., R449E) greatly reduced affinity for PtdIns(4,5)P_2-containing vesicles (Figure S7C). Furthermore, none of these mutations decreased binding to the C-terminal peptide of stargazin, an interaction partner of SAP-102 (Figure S7D). Thus, this PDZ domain has a relatively well-formed binding site for

Table 2. Experimental Evaluation of Our Prediction for Membrane Binding of PDZ Domains

Domain	Species	Residue Number	K_d (nM) for PM	Prediction
C2PA-PDZ1	mouse	185–271	NM[a]	−0.20
Chapsyn110-PDZ1	rat	98–182	NM	−1.70
Chapsyn110-PDZ2	rat	193–277	510 ± 50[b]	0.17
GRIP-PDZ3	rat	252–333	NM	−0.30
GRIP-PDZ4	rat	471–557	NM	−0.30
GRIP-PDZ5	rat	572–654	NM	0.00
GRIP-PDZ6	rat	672–751	NM	−0.70
InaD-PDZ1	fruit fly	17–103	NM	−0.30
MUPP1-PDZ10	mouse	1,614–1,697	NM	−0.2
PAPIN-PDZ1	rat	85–177	NM	−0.30
PAR3-PDZ1	rat	271–359	NM	***0.05***
PAR3-PDZ3	rat	590–681	NM	−0.06
PTPN3-PDZ1	human	510–595	450 ± 90	0.60
PTPN13-PDZ1	mouse	1,084–1,167	NM	−0.10
Rhophilin-2-PDZ	human	515–593	500 ± 30	0.37
SAP102-PDZ2	rat	244–328	NM	−0.50
Shank1-PDZ1	rat	663–754	NM	−0.40
ZO-1 PDZ-1	mouse	23–107	NM	−0.70
ZO-1 PDZ-3	mouse	421–502	NM	−0.70
ZO-2 PDZ-1	mouse	10–94	NM	−0.90
ZO-2 PDZ-2	mouse	287–365	1200 ± 400	***0.10***
ZO-2 PDZ-3	mouse	489–570	NM	−0.40
ZO-3 PDZ-1	mouse	11–90	NM	−0.20
ZO-3 PDZ-2	mouse	187–261	NM	***0.10***
ZO-3 PDZ-3	mouse	370–448	NM	−0.20

The prediction values were calculated using the 1 μM K_d-SVM model. Positive values indicate membrane binding, whereas negative values indicate nonbinding. The further away from zero, the more confident the prediction is. Prediction values for three misclassified cases were shown in bold italic.

[a]Not measurable by SPR analysis (i.e, K_d >10 μM).

[b]Mean ±SD values determined by SPR analysis using PM-mimetic vesicles (i.e, K_d >10 μM).

PtdIns(4,5)P_2 and PtdIns(3,4,5)P_3 that is distant from the peptide-binding pocket, and it can simultaneously bind a PtdIns(4,5)P_2 (or PtdIns[3,4,5]P_3) and a protein molecule (see Figure 3A). The list of class A PDZ domains with a well-formed cationic groove and thus with potential lipid head group specificity is shown in Table S3. Based on our results, we postulate that class A PDZ domains have topologically distinct and functionally orthogonal lipid- and protein-binding sites. This notion is supported by functionally independent lipid and peptide-binding sites observed for two additional members of the class A family, PICK1-PDZ (Pan et al., 2007) and NHERF1-PDZ1 (R.S., Y.C., H.Y. Gee, P.J. Lee, H.R. Melowic, E. Stec, N.R. Blatner, M.P. Tun, M.K., T.K. Fujiwara, H.L., A. Kusumi, M.G. Lee, and W.C., unpublished data).

To directly determine the interplay between lipid and peptide binding of class A PDZ domains, we quantified the binding

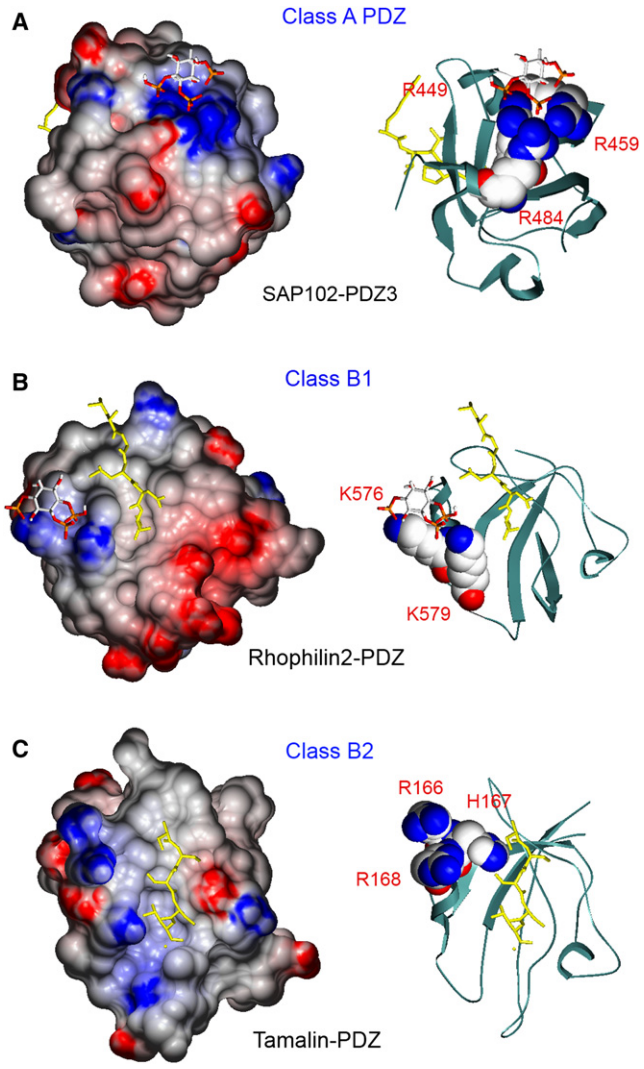

Figure 3. Functional Classification of Membrane-Binding PDZ Domains

(A) The energy-minimized model structure of the SAP102-PDZ3-peptide(RTTPV)-Ins(1,4,5)P_3 ternary complex. Electrostatic surface potential (left) and the ribbon diagram (right) show the separation of the peptide- and lipid-binding sites. In the ribbon diagram, R449, R459, and R484 that form the cationic groove are shown in space-filling representation and labeled.

(B) The energy-minimized model structure of the rhophilin 2-PDZ-peptide(EYLGLDVPV)-Ins(1,4,5)P_3 ternary complex. Electrostatic surface potential (left) and the ribbon diagram (right) show the proximity of the peptide- and lipid-binding sites. In the ribbon diagram, K576 and K579 in the α2A helix that are involved in lipid binding are shown in space-filling representation and labeled.

(C) The energy-minimized model structure of tamalin-PDZ-peptide (IRDYTQSSSSL) binary complex. Because of severe steric clash, an Ins(1,4,5)P_3 molecule could not be docked on the PDZ-peptide complex. In the ribbon diagram, R166, H167, and R168 in the α2A helix that constitute the lipid-binding site are shown in space-filling representation and labeled. Electrostatic calculations were performed using GRASP2 (Petrey and Honig, 2003). Blue and red colors indicate positive and negative electrostatic potential, respectively. See the Supplemental Experimental Procedures for molecular docking procedures.

between SAP102-PDZ3 and the N-fluorescein-labeled stargazin peptide in the presence and absence of PM vesicles (notice that they contain 1% PtdIns[4,5]P_2 for which SAP102-PDZ3 shows selectivity) by fluorescence anisotropy measurements. As shown in Figure 4A, the presence of PM vesicles had little effect on the peptide binding of SAP102-PDZ3. Since a significant portion of the PDZ domain was vesicle bound under these experimental conditions, the result verifies the notion that SAP102-PDZ3 can simultaneously bind the membrane and a protein molecule. Also, PM vesicles did not affect the binding of SAP102-PDZ3 to other peptides (see Table S4), indicating that lipid binding of the class A PDZ domain does not directly modulate its protein specificity.

Class B PDZ domains typically have cationic residues clustered around the α2A helix that forms a wall of the peptide-binding pocket (Figure S6). Some PDZ domains belonging to this group have been reported to have partially overlapping (Zimmermann et al., 2002) or mutually exclusive (Meerschaert et al., 2009) lipid- and peptide-binding sites. Since the peptide and lipid-binding modes of PDZ domains can vary significantly, however, it is difficult to predict the degree of functional overlap between the two sites based solely on structural examination. We therefore selected two members (rhophilin 2-PDZ and tamalin-PDZ) of this family and determined the location of their lipid-binding sites and the degree of their overlap with respective peptide-binding sites. Rhophilin 2-PDZ interacts nonspecifically with anionic lipids, including PtdIns*P*s. It has two cationic residues (K576 and K579) on the same side of the α2A near its C-terminal end (Figure 3B and Figure S6) that may be involved in anionic lipid binding. As shown in Figure 5A, double-site mutations of K576 and K579 (i.e., K576A/K579A or K576E/K579E) greatly reduced the affinity of rhophilin 2-PDZ for PM vesicles, suggesting their direct involvement in binding to anionic membranes. Interestingly, these mutants bind the C-terminal peptide of ErbB2 as well as the wild-type (WT), suggesting that the lipid-binding site does not overlap with the peptide-binding site (Figure 5B). We identified this peptide as the best binding partner for the rhophilin 2-PDZ through screening a small library of PDZ domain-binding peptides, because its physiological binding partners have not been reported. Our molecular modeling also supports the notion that rhophilin 2-PDZ can simultaneously interact with an anionic lipid head group and a peptide (Figure 3B). To rigorously test the functional independence of lipid- and peptide-binding sites of rhophilin 2-PDZ, we measured the binding between rhophilin 2-PDZ and the N-fluorescein-labeled peptides in the presence and absence of PM vesicles by fluorescence anisotropy analysis (Figure 4B and Table S4). Interestingly, the presence of PM vesicles caused a 2-fold increase in the affinity of rhophilin 2-PDZ for the ErbB2 peptide while modestly (i.e., <1.8-fold) decreasing the affinity for other peptides. Thus, neighboring lipid- and peptide-binding sites of rhophilin 2-PDZ can interact with their binding partners simultaneously, but unlike the case of class A PDZ domains, its lipid binding may enhance the specificity of protein binding. A similar pattern of the interplay between neighboring lipid- and peptide-binding sites was also seen in Dvl2-PDZ (R.S., Y.C., H.Y. Gee, P.J. Lee, H.R. Melowic, E. Stec, N.R. Blatner, M.P. Tun, M.K., T.K. Fujiwara, H.L., A. Kusumi, M.G. Lee, and

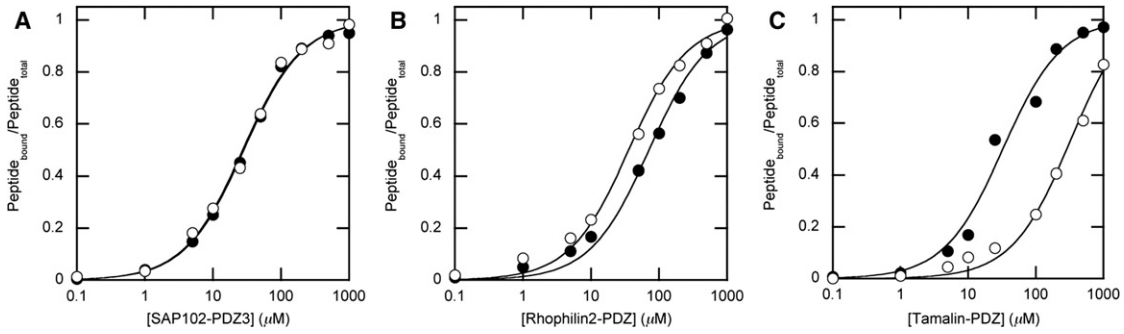

Figure 4. Effects of Lipid Binding of Each Class of the PDZ Domain on Its Peptide Binding

(A) Binding of class A SAP102-PDZ3 to F-Ahx-RTTPV in the absence (filled symbols) and presence (open symbols) of 150 μM PM-mimetic vesicles.
(B) Binding of class B_1 rhophilin 2-PDZ to F-Ahx-EYLGLDVPV in the absence (filled symbols) and presence (open symbols) of 150 μM PM-mimetic vesicles.
(C) Binding of class B_2 tamalin-PDZ to F-Ahx-IRDYTQSSSSL in the absence (filled symbols) and presence (open symbols) of 150 μM PM-mimetic vesicles. The peptide concentration was 5 nM. Notice that for the class A and B_1 PDZ domains, vesicles have a modest to no effect on peptide binding, whereas for the class B_2 PDZ domain, vesicles greatly interfere with the peptide binding. See Table S4 for K_d values and the Experimental Procedures for experimental details.

W.C., unpublished data). We thus designated this subgroup of class B PDZ domains as class B_1.

The crystal structure of tamalin-PDZ showed that two phosphate ions are bound to the N-terminal end of the α2A, suggesting that three cationic residues, R166, H167, and R168, are involved in anionic lipid binding (Sugi et al., 2008). We found that tamalin-PDZ also lacks definite PtdIns*P* specificity (Figure S9A). Mutation of any of the cationic residues to A or E reduced its binding to the PM-mimetic (or PtdIns*P*-containing) membranes, supporting the notion that these residues are involved in nonspecific anionic lipid binding (Figure S9B). Unlike the case of rhophilin 2, however, these mutants showed greatly reduced binding to the C-terminal peptide of mGluR5, an interaction partner of tamalin, indicating a significant degree of overlap between the two binding sites (Figure S9C), which is consistent with molecular modeling (see Figure 3C). The functional overlap between the two binding sites is further verified by the finding that the presence of PM vesicles significantly reduced the binding of tamalin-PDZ to the N-terminal fluorescein-labeled mGluR5 peptide (Figure 4C) and other peptides (Table S4). To distinguish these PDZ domains from rhophilin-like class B_1 PDZ domains, we designate them class B_2 PDZ domains. Together, these results show that our systematic structural analysis can predict the location of the lipid-binding site of PDZ domains with high accuracy. For class A PDZ domains, lipid- and peptide-binding sites are topologically distinct and functionally orthogonal, but for those class B PDZ domains with neighboring lipid- and peptide-binding sites, functional analysis is required to determine the interplay of lipid and peptide binding. Our analysis can also identify those PDZ domains (mostly class A) with a relatively well-defined lipid-binding pocket and hence with lipid specificity.

Physiological Significance of Membrane Binding of PDZ Domains

Physiological roles of the lipid-binding activity of class A (Pan et al., 2007) and class B_2 (Meerschaert et al., 2009; Zimmermann et al., 2002) PDZ domains have been reported. However, the physiological significance of lipid-binding activity of class B_1 PDZ domains has not been established, presumably due to the subtle nature of the interplay between lipid and protein binding for these PDZ domains. We thus selected rhophilin 2-PDZ, a prototypical class B_1 PDZ domain with modest membrane affinity (i.e. K_d = 500 nM), and performed cell studies to determine how lipid binding controls its cellular activity. Rhophilin 2 is a single PDZ domain-containing RhoA-binding protein that inhibits the RhoA's activity to induce F-actin stress fibers (Peck et al., 2002; Watanabe et al., 1996). It was reported that overexpression of rhophilin 2 in HeLa cells caused disassembly of F-actin stress fibers and that this activity required the presence of its PDZ domain (Peck et al., 2002). When the full-length rhophilin 2 (or its PDZ domain) was expressed as a monomeric red fluorescence protein (mRFP)-fusion protein in HeLa cells, it showed membrane localization with predominant distribution at the perinuclear region and the PM (Figure 5C). Most important, the cells expressing rhophilin 2 exhibited distinct morphology with dramatically reduced stress fibers, confirming the reported function of rhophilin 2. As illustrated in Figures 5D and 5E, K576A/K579A and K576E/K579E with reduced membrane affinity show primarily cytosolic distribution with little membrane localization, although they have intact protein-binding activity (Figure 5B). Furthermore, both mutations abrogated the activity of rhophilin 2 to disassemble stress fibers, as all mutant-expressing cells contain as many stress fibers as control cells (Figure 5F). Thus, it is evident that lipid binding of rhophilin 2-PDZ is important for the physiological function of rhophilin 2. These results, in conjunction with previous reports on class A and class B_2 PDZ domains, suggest that lipid-binding activity of all three classes of lipid-binding PDZ domains is important for physiological function and regulation of their host proteins.

DISCUSSION

This study describes genome-wide identification, characterization, and classification of membrane-binding PDZ domains. Experimental characterization of 95 PDZ domains confirms

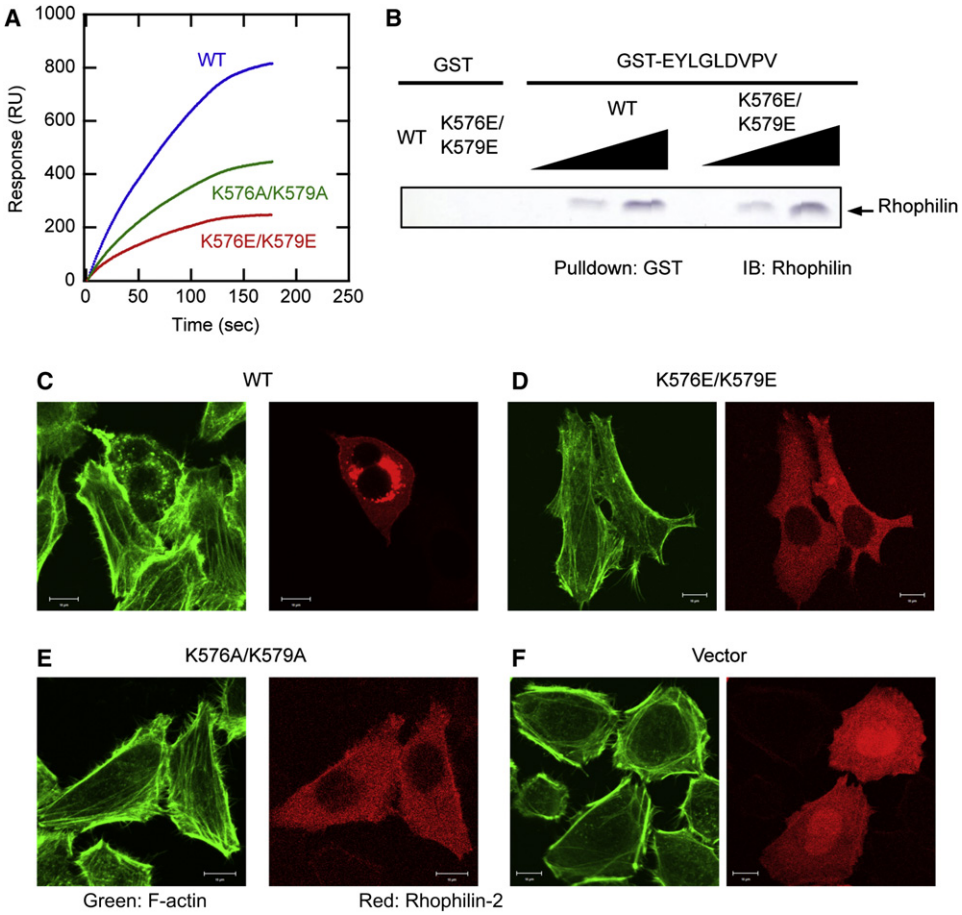

Figure 5. Effects of Lipid Binding of Rhophilin 2-PDZ on the Cellular Localization and Function of Rhophilin 2

(A) Membrane binding of rhophilin 2-PDZ WT and mutants. Binding of PDZ domains to PM-mimetic vesicles was measured by SPR analysis. The two mutants show significantly reduced membrane affinity.

(B) GST pull-down assay for rhophilin 2-PDZ WT and K576E/K579E. GST or GST-EYLGLDVPV (5 μg) was incubated with 0–5 μg of rhophilin 2 proteins, and the GST-bound proteins were analyzed by SDS-PAGE and immunoblotting by a rhophilin 2 antibody.

(C) Confocal microscopic images of F-actin (green) and rhophilin 2 (red) in fixed HeLa cells transiently transfected with mRFP-tagged rhophilin 2 WT. Notice that only the rhophilin 2-expressing cell shows distinct morphology and dramatically reduced F-actin stress fibers.

(D and E) Confocal images for K576A/K579A and K576E/K579E mutants, respectively. These mutants show distinctly different subcellular localization patterns from WT and have little effect on F-actin.

(F) The control images taken using HeLa cells transfected with the empty expression vector. White bars indicate 10 μm.

that membrane binding is a common property of PDZ domains. Our quantitative data reveal that PDZ domains have a wide continuous range (i.e., 20 nM to >10 μM) of affinity for PM vesicles, making it difficult to arbitrarily distinguish membrane-binding domains from nonbinding ones. This also underscores the risk of identifying membrane-binding PDZ domains by a qualitative assay. Taking this factor into account, we developed a flexible and robust binary classification strategy in which a threshold or cut-off K_d value is arbitrarily set and the domains are then divided into those with higher affinity (binding) and those with lower affinity (nonbinding). Our online resource provides an option to set the threshold K_d value as a variable, and one can thus predict the membrane-binding activity of PDZ domains with flexibility. Our new classification and prediction protocols represent a major advancement in bioinformatics computation, because they allow accurate prediction of membrane-binding proteins from a group of proteins with high sequence and structural similarity. The same methodology can be applied to the prediction of any other membrane-binding PIDs that might act as dual-specificity protein- and lipid-binding modules.

A recent study indicated that at least 80% of mouse PDZ domains have protein (or peptide)-binding activity (Stiffler et al., 2007). Given that ~30% of mouse PDZ domains have submicromolar affinity for the PM membrane, the probability that a mouse PDZ domain is a lipid- and protein-binding dual-specificity module is >24%. Also, if a PDZ domain is found to bind membranes, the probability that it can also bind proteins is >90%. These are conservative estimates, and actual numbers might well be higher for PDZ domains from mouse and other species. Thus, it is safe to state that almost all lipid-binding

PDZ domains are dual-specificity modules. To gain insight into the evolution of lipid- and protein-binding activities of PDZ domains, we constructed a dendrogram depicting the evolutionary relationship of a collection of PDZ domains (Figure S10). The dendrogram shows that the binding to specific protein classes is well preserved in the tree, whereas membrane-binding properties vary even for evolutionarily closely related PDZ domains (e.g., Dvl and SAP97/PSD95/Chapsyn110 clusters). Also, most PDZ domains have peptide-binding activity, and the location of their peptide-binding pockets is essentially invariable (Sheng and Sala, 2001), while they show a wide range of membrane-binding activity and the locations of their lipid-binding sites are highly variable. These findings all suggest that dual-specificity lipid- and protein-binding PDZ domains evolved from protein-binding ancestor PDZ domains through convergent evolution. Newly acquired lipid-binding activity should confer additional functionality to PDZ domains and also allow an extra layer of regulation on the critical cellular functions of their host proteins.

Systematic and comprehensive electrostatic potential calculation of membrane-binding PDZ domains reveals two distinct patterns of cationic patch distribution, allowing for their classification into two groups. Mutational and functional analysis confirmed that class A PDZ domains have topologically distinct and functionally orthogonal lipid and protein-binding sites. Thus, these PDZ domains can serve as dual-specificity lipid- and protein-binding modules that mediate membrane-associated protein networking through coincident binding. Also, many class A PDZ domains have a relatively well-formed cationic groove (Figure S5 and Table S3), suggesting that they have definite lipid head group selectivity (Table 1), in contrast to most class B PDZ domains with low lipid selectivity. Our results show that lipid binding of class A PDZ domains affects neither affinity nor specificity per se for peptide binding. Under physiological conditions, however, their lipid binding should enhance affinity and specificity for their protein partners, many of which are PM-associated proteins, due to reduction in dimensionality (Cho, 2006; McCloskey and Poo, 1986). Thus, their dual specificity should be pivotal for the formation and regulation of membrane-associated protein networking.

Essentially all class B PDZ domains have their prominent cationic patches in or near the α2A helix that forms a wall of the peptide-binding pocket. Interestingly, class B_1 PDZ domains have cationic patches confined near the C-terminal end of the α2A helix, whereas class B_2 PDZ domains have cationic patches in the N-terminal end of the helix or scattered over the helix (Figure S7). Since a protein typically enters the pocket from the N-terminal end of the α2A helix to place its C terminus near the carboxylate-binding loop, it is possible that lipid binding at the N-terminal end of the α2A helix interferes with the protein binding more than that at the C-terminal end of the helix. Further characterization of class B PDZ domains would undoubtedly expand the list of class B_1 PDZ domains and also reveal if the distribution of cationic residues in the α2A is the main determinant for class B_1 PDZ domains. Class B_1 PDZ domains are similar to class A PDZ domains in that both act as dual-specificity modules that mediate membrane-associated protein networking through coincident binding. Unlike the case of class A PDZ domains, however, lipid binding may enhance the protein binding specificity of class B_1 PDZ domains, presumably through a local conformational change of the peptide-binding pocket. Undoubtedly, further studies are necessary to test this potentially important notion. Since lipid and peptide binding are mutually exclusive and compete with each other for class B_2 PDZ domains, lipid binding should negatively control their protein binding; i.e., lipids may act as a molecular switch that regulates the accessibility of the protein-binding pocket.

The main regulatory role of lipids is modulation of the localization and the activity of proteins. Thus, lipid binding of PDZ domains would primarily control the membrane localization and/or the activity of their host proteins. For most reported class A and class B_2 PDZ domains, their lipid-binding activity appears to be important for the cellular localization of their host proteins. Our results from rhophilin 2 containing a class B_1 PDZ domain would seem to indicate that this is the common feature of all dual-specificity PDZ domains. However, the correlation between membrane affinity (i.e., PM affinity) and cellular membrane localization may not be straightforward, because their membrane localization may also depend on interactions with membrane proteins or membrane-associated proteins. In the case of the yeast scaffold protein Ste5, lipid binding was reported to modulate the dynamics and function of the protein at the PM rather than PM localization per se (Winters et al., 2005). Likewise, lipid binding of some PDZ domains may exert more effects on the dynamics and function of their host proteins at the membrane than on their membrane localization. Also, some PDZ domains are found associated with intracellular organelles (Meerschaert et al., 2009; Zimmermann et al., 2002), suggesting that PDZ domains may interact with other cellular membranes. In any case, however, our experimental and predicted PM affinity should still serve as a reliable indicator of the likelihood of a PDZ domain to interact with any cell membrane, because the electrostatic interaction between the PDZ domain and anionic lipids is the main driving force for its binding to all intracellular cell membranes. Lastly, it should be noted that some PDZ domains may hetero- or homodimerize (or oligomerize) under physiological conditions (Feng and Zhang, 2009; Sheng and Sala, 2001), which may modulate their effective membrane affinity through avidity or conformational effect.

Taken all together, our results strongly support the hypothesis that many PIDs involved in protein networking at the membrane serve as dual-specificity lipid- and protein-interaction modules. Also, lipid binding of different classes of PDZ domains regulates the cellular function and regulation of their host proteins by different mechanisms. Thus, it is becoming increasingly evident that the interpretation of complex data on the regulation of cellular protein interactions and networking entails elucidation of the membrane-binding properties of PIDs. Our experimental and computational data on PDZ domains should serve as a valuable resource not only for those investigators working on PDZ domain proteins but also for other proteins that mediate cellular protein interactions and networking. Also, our structure-based functional classification approach should provide a framework for further functional characterization of all dual-specificity PDZ domains and other PIDs.

EXPERIMENTAL PROCEDURES

Protein Expression and Purification

All PDZ domains were expressed as His_6-tagged proteins in *Escherichia coli* BL21 (DE3) pLysS (Novagen). For details, see the Supplemental Experimental Procedures.

Lipid Vesicle Preparation and SPR Analysis

PM-mimetic vesicles were prepared by mixing 1-palmitoyl-2-oleoyl-*sn*-glycero-3-phosphocholine (POPC), 1-palmitoyl-2-oleoyl-*sn*-glycero-3-phosphoethanolamine, 1-palmitoyl-2-oleoyl-*sn*-glycero-3-phosphoserine, cholesterol, liver phosphoinositol, and 1,2-dipalmitoyl derivatives of phosphatidylinositol-(4,5)-bisphosphate in a molar ratio of 12:35:22:22:8:1. Large unilamellar vesicles were prepared using a Liposofast (Avestin) microextruder with a 100 nm polycarbonate filter. All SPR measurements were performed at 23°C using a lipid-coated L1 chip in the BIACORE X system as described (Stahelin and Cho, 2001). PM-mimetic vesicles and POPC vesicles were coated on the active surface and the control surface, respectively, and 20 mM Tris-HCl (pH 7.4) containing 0.16 M NaCl was used as the running buffer. For details, see the Supplemental Experimental Procedures.

Mammalian Cell Assay

HeLa cells were maintained in minimum essential medium Eagle's medium (MEME) supplemented with 10% fetal bovine serum at 37°C in 10% CO_2. Cells were transiently transfected with 0.5 μg of appropriate plasmid DNA using Lipofectamine Plus (Invitrogen). After 18 hr, the cells were fixed using 4% formaldehyde solution, and the F-actin was stained using Oregon Green 488-conjugated phalloidin (Invitrogen). Images were taken using a Zeiss LSM510 confocal microscope.

Screening of Rhophilin 2-PDZ-Binding Peptides

Since physiological binding partners for the rhophilin 2-PDZ domain are unknown, we constructed a small library of PDZ domain-binding peptides and screened them against the rhophilin 2-PDZ. The library contains several representative C-terminal nonapeptides for each class of PDZ domains with differential peptide specificity (Sheng and Sala, 2001); i.e., neuroligin (PSD95-PDZ3-specific), CFTR (NHERF1-PDZ1-specific), and Frizzled7 (Dvl2-PDZ-specific) for class I PDZ domains; GluR2 (GRIP-PDZ5-specific) and ErbB2 (erbin-PDZ-specific) for class II PDZ domains; and melatonin receptor (nNOS-PDZ-specific) and merlin (syntenin PDZ1-specific) for class III PDZ domains. The GST pull-down and immunoblotting assay showed that rhophilin 2-PDZ had high selectivity for the C-terminal peptide of ErbB2, EYLGLDVPV.

PDZ-Peptide-Binding Assay by Fluorescence Anisotropy

Fluorescein-6-aminohexanoyl (F-Ahx)-labeled peptides, F-Ahx-RTTPV (for SAP102-PDZ binding), F-Ahx-EYLGLDVPV (for rhophilin 2-PDZ binding), and F-Ahx-IRDYTQSSSSL (for tamalin-PDZ binding) were dissolved in 20 mM Tris buffer (pH 7.9) containing 160 mM NaCl, 300 mM imidazole, and 5% dimethylsulfoxide. To each well of a 96-well flat bottom black polystyrol plate was added 100 μl solution containing each peptide (5 nM) and PDZ domain (100 nM to 1 mM) with or without 150 μM PM vesicles. After 30 min incubation, the plate was inserted into Tecan Genios Pro spectrofluorometer, and the fluorescence anisotropy (r) was measured with excitation and emission wavelengths set at 485 and 535 nm, respectively. Since $P_o \gg Pep_o$ under our conditions, the K_d for the PDZ domain-peptide binding was determined by the nonlinear least-squares analysis of the binding isotherm using the equation

$$\frac{Pep_{bound}}{Pep_o} = \frac{\Delta r}{\Delta r_{max}} = \frac{1}{1 + K_d/P_o}$$

where Pep_{bound}, Pep_o, and P_o indicate the concentration of bound peptide, total peptide, and total PDZ domain, respectively, and Δr and Δr_{max} are the anisotropy change for each P_o and the maximal Δr, respectively.

Bioinformatics Methods, Molecular Docking, and Calculation of Electrostatic Potential

Detailed descriptions for feature calculations, classifiers, classifier evaluations, homology modeling, and electrostatic potential calculation with GRASP2 (Petrey and Honig, 2003) are included in the Supplemental Experimental Procedures.

SUPPLEMENTAL INFORMATION

Supplemental information includes ten figures, four tables, Supplemental Experimental Procedures, and Supplemental References and can be found with this article online at doi:10.1016/j.molcel.2012.02.012.

ACKNOWLEDGMENTS

This work was in part supported by the Chicago Biomedical Consortium with support from The Searl Funds at the Chicago Community Trust and the National Institutes of Health (GM68849 for W.C., GM094597-01 and CA121852-07 for B.H., and NS072394 for R.A.H.). The work was also supported by the World Class University program R31-2008-000-10105-0 (W.C.) through the National Research Foundation of Korea funded by the Ministry of Education, Science, and Technology. M.K. thanks FMC Technologies Fund Fellowship for support. W.C. thanks Dr. Soo Hyun Eom for the generous gift of PDZ domain constructs.

Received: July 15, 2011
Revised: December 2, 2011
Accepted: February 24, 2012
Published online: March 22, 2012

REFERENCES

Bhardwaj, N., Langlois, R.E., Zhao, G., and Lu, H. (2005). Kernel-based machine learning protocol for predicting DNA-binding proteins. Nucleic Acids Res. *33*, 6486–6493.

Bhardwaj, N., Stahelin, R.V., Langlois, R.E., Cho, W., and Lu, H. (2006). Structural bioinformatics prediction of membrane-binding proteins. J. Mol. Biol. *359*, 486–495.

Bhardwaj, N., Stahelin, R.V., Zhao, G., Cho, W., and Lu, H. (2007). MeTaDoR: a comprehensive resource for membrane targeting domains and their host proteins. Bioinformatics *23*, 3110–3112.

Bhattacharyya, R.P., Remenyi, A., Yeh, B.J., and Lim, W.A. (2006). Domains, motifs, and scaffolds: the role of modular interactions in the evolution and wiring of cell signaling circuits. Annu. Rev. Biochem. *75*, 655–680.

Blatner, N.R., Stahelin, R.V., Diraviyam, K., Hawkins, P.T., Hong, W., Murray, D., and Cho, W. (2004). The molecular basis of the differential subcellular localization of FYVE domains. J. Biol. Chem. *279*, 53818–53827.

Bray, D. (1998). Signaling complexes: biophysical constraints on intracellular communication. Annu. Rev. Biophys. Biomol. Struct. *27*, 59–75.

Cho, W. (2006). Building signaling complexes at the membrane. Sci. STKE *2006*, pe7.

Cho, W., and Stahelin, R.V. (2005). Membrane-protein interactions in cell signaling and membrane trafficking. Annu. Rev. Biophys. Biomol. Struct. *34*, 119–151.

Cho, W., Bittova, L., and Stahelin, R.V. (2001). Membrane binding assays for peripheral proteins. Anal. Biochem. *296*, 153–161.

DiNitto, J.P., and Lambright, D.G. (2006). Membrane and juxtamembrane targeting by PH and PTB domains. Biochim. Biophys. Acta *1761*, 850–867.

DiNitto, J.P., Cronin, T.C., and Lambright, D.G. (2003). Membrane recognition and targeting by lipid-binding domains. Sci. STKE *2003*, re16.

Di Paolo, G., and De Camilli, P. (2006). Phosphoinositides in cell regulation and membrane dynamics. Nature *443*, 651–657.

Feng, W., and Zhang, M. (2009). Organization and dynamics of PDZ-domain-related supramodules in the postsynaptic density. Nat. Rev. Neurosci. *10*, 87–99.

Lee, C.S., Kim, I.S., Park, J.B., Lee, M.N., Lee, H.Y., Suh, P.G., and Ryu, S.H. (2006). The phox homology domain of phospholipase D activates dynamin GTPase activity and accelerates EGFR endocytosis. Nat. Cell Biol. *8*, 477–484.

Lemmon, M.A. (2008). Membrane recognition by phospholipid-binding domains. Nat. Rev. Mol. Cell Biol. *9*, 99–111.

McCloskey, M.A., and Poo, M.M. (1986). Rates of membrane-associated reactions: reduction of dimensionality revisited. J. Cell Biol. *102*, 88–96.

McLaughlin, S., and Murray, D. (2005). Plasma membrane phosphoinositide organization by protein electrostatics. Nature *438*, 605–611.

Meerschaert, K., Tun, M.P., Remue, E., De Ganck, A., Boucherie, C., Vanloo, B., Degeest, G., Vandekerckhove, J., Zimmermann, P., Bhardwaj, N., et al. (2009). The PDZ2 domain of zonula occludens-1 and -2 is a phosphoinositide binding domain. Cell. Mol. Life Sci. *66*, 3951–3966.

Mulgrew-Nesbitt, A., Diraviyam, K., Wang, J., Singh, S., Murray, P., Li, Z., Rogers, L., Mirkovic, N., and Murray, D. (2006). The role of electrostatics in protein-membrane interactions. Biochim. Biophys. Acta *1761*, 812–826.

Pan, L., Wu, H., Shen, C., Shi, Y., Jin, W., Xia, J., and Zhang, M. (2007). Clustering and synaptic targeting of PICK1 requires direct interaction between the PDZ domain and lipid membranes. EMBO J. *26*, 4576–4587.

Park, W.S., Heo, W.D., Whalen, J.H., O'Rourke, N.A., Bryan, H.M., Meyer, T., and Teruel, M.N. (2008). Comprehensive identification of PIP3-regulated PH domains from *C. elegans* to *H. sapiens* by model prediction and live imaging. Mol. Cell *30*, 381–392.

Pawson, T. (2004). Specificity in signal transduction: from phosphotyrosine-SH2 domain interactions to complex cellular systems. Cell *116*, 191–203.

Pawson, T., and Nash, P. (2003). Assembly of cell regulatory systems through protein interaction domains. Science *300*, 445–452.

Peck, J.W., Oberst, M., Bouker, K.B., Bowden, E., and Burbelo, P.D. (2002). The RhoA-binding protein, rhophilin-2, regulates actin cytoskeleton organization. J. Biol. Chem. *277*, 43924–43932.

Petrey, D., and Honig, B. (2003). GRASP2: visualization, surface properties, and electrostatics of macromolecular structures and sequences. Methods Enzymol. *374*, 492–509.

Ravichandran, K.S., Zhou, M.M., Pratt, J.C., Harlan, J.E., Walk, S.F., Fesik, S.W., and Burakoff, S.J. (1997). Evidence for a requirement for both phospholipid and phosphotyrosine binding via the Shc phosphotyrosine-binding domain in vivo. Mol. Cell. Biol. *17*, 5540–5549.

Schultz, J., Milpetz, F., Bork, P., and Ponting, C.P. (1998). SMART, a simple modular architecture research tool: identification of signaling domains. Proc. Natl. Acad. Sci. USA *95*, 5857–5864.

Sheng, M., and Sala, C. (2001). PDZ domains and the organization of supramolecular complexes. Annu. Rev. Neurosci. *24*, 1–29.

Stahelin, R.V., and Cho, W. (2001). Differential roles of ionic, aliphatic, and aromatic residues in membrane-protein interactions: a surface plasmon resonance study on phospholipases A2. Biochemistry *40*, 4672–4678.

Stahelin, R.V., Long, F., Peter, B.J., Murray, D., De Camilli, P., McMahon, H.T., and Cho, W. (2003). Contrasting membrane interaction mechanisms of AP180 N-terminal homology (ANTH) and epsin N-terminal homology (ENTH) domains. J. Biol. Chem. *278*, 28993–28999.

Stiffler, M.A., Chen, J.R., Grantcharova, V.P., Lei, Y., Fuchs, D., Allen, J.E., Zaslavskaia, L.A., and MacBeath, G. (2007). PDZ domain binding selectivity is optimized across the mouse proteome. Science *317*, 364–369.

Sugi, T., Oyama, T., Morikawa, K., and Jingami, H. (2008). Structural insights into the PIP2 recognition by syntenin-1 PDZ domain. Biochem. Biophys. Res. Commun. *366*, 373–378.

Watanabe, G., Saito, Y., Madaule, P., Ishizaki, T., Fujisawa, K., Morii, N., Mukai, H., Ono, Y., Kakizuka, A., and Narumiya, S. (1996). Protein kinase N (PKN) and PKN-related protein rhophilin as targets of small GTPase Rho. Science *271*, 645–648.

White, S.H., Wimley, W.C., Ladokhin, A.S., and Hristova, K. (1998). Protein folding in membranes: determining energetics of peptide-bilayer interactions. Methods Enzymol. *295*, 62–87.

Winters, M.J., Lamson, R.E., Nakanishi, H., Neiman, A.M., and Pryciak, P.M. (2005). A membrane binding domain in the ste5 scaffold synergizes with gbetagamma binding to control localization and signaling in pheromone response. Mol. Cell *20*, 21–32.

Wu, H., Feng, W., Chen, J., Chan, L.N., Huang, S., and Zhang, M. (2007). PDZ domains of Par-3 as potential phosphoinositide signaling integrators. Mol. Cell *28*, 886–898.

Yao, L., Kawakami, Y., and Kawakami, T. (1994). The pleckstrin homology domain of Bruton tyrosine kinase interacts with protein kinase C. Proc. Natl. Acad. Sci. USA *91*, 9175–9179.

Yoon, Y., Lee, P.J., Kurilova, S., and Cho, W. (2011). In situ quantitative imaging of cellular lipids using molecular sensors. Nat. Chem. *3*, 868–874.

Zhou, M.M., Ravichandran, K.S., Olejniczak, E.F., Petros, A.M., Meadows, R.P., Sattler, M., Harlan, J.E., Wade, W.S., Burakoff, S.J., and Fesik, S.W. (1995). Structure and ligand recognition of the phosphotyrosine binding domain of Shc. Nature *378*, 584–592.

Zimmermann, P. (2006). The prevalence and significance of PDZ domain-phosphoinositide interactions. Biochim. Biophys. Acta *1761*, 947–956.

Zimmermann, P., Meerschaert, K., Reekmans, G., Leenaerts, I., Small, J.V., Vandekerckhove, J., David, G., and Gettemans, J. (2002). PIP(2)-PDZ domain binding controls the association of syntenin with the plasma membrane. Mol. Cell *9*, 1215–1225.